ELSEVIER

Journal of Photochemistry and Photobiology A: Chemistry 114 (1998) 145–150

Journal of Photochemistry and Photobiology A:Chemistry

A steady state fluorescence study of nonamphiphilic *N,N'*-bis(2,6-dimethylphenyl)-3,4,9,10-perylenetetracarboxylic diimide in supramolecular Langmuir–Blodgett assemblies

A.K. Dutta *

GREIB, Departement de Chimie-Biologie, Universite du Quebec à Trois-Rivieres, C.P. 500, Trois-Rivieres, Quebec, Canada G9A 5H7

Received 5 June 1997; received in revised form 19 November 1997; accepted 4 December 1997

Abstract

This paper reports the behavior of mixed films of nonamphiphilic *N,N'*-bis(2,6-dimethylphenyl)-3,4,9,10-perylenetetracarboxylic diimide (DMPI) and stearic acid (SA) at the air–water interface studied by conventional surface pressure vs. area per molecule isotherms. Pure DMPI formed stable films at the air–water interface, nevertheless, these films were untransferable onto solid substrates. However, mixed films of DMPI with SA at the air–water interface were highly stable and could be easily transferred onto solid substrates as Langmuir–Blodgett (LB) films. Steady state absorption and fluorescence emission studies of these films show broadening and red shift in their spectral profiles when compared to the absorption and emission spectra of DMPI in solution, indicating the formation of organized aggregates in the LB films. Perhaps the most interesting feature revealed in this study is a broad excimer-like emission that may be attributed to the formation of a loosely bound dimer. Aggregation of DMPI molecules induced in binary solvent mixtures of acetone and water is observed to produce identical results. A comparative study of the spectroscopic characteristics of the aggregates in the LB films, binary solvent mixtures and microcrystals yielded identical results confirming the formation of microcrystalline domains in the mixed LB films.

Keywords: Langmuir–Blodgett films; Perylenetetracarboxylic diimide; Aggregation; Fluorescence spectroscopy

1. Introduction

In recent years, considerable attention has been focused on the study of dyes and pigments incorporated in Langmuir–Blodgett (LB) films to meet the desired requirements for ultrafast, miniaturized, optoelectronic and photonic devices [1–3]. Large polyaromatic hydrocarbons (PAHs) with condensed ring systems are considered to be attractive for this purpose as in addition to these molecules being intensely fluorescent, they exhibit excellent soliton and photoconducting properties [4].

Perylene and its derivatives meet many of the above mentioned requirements and have been recently used in the preparation of thin film p–n heterojunctions [5], rectifiers [6], liquid crystal displays [7], electroluminescent [8], and xerographic [9] devices. The carboxyimide derivatives of perylene are of special interest owing to their extended condensed ring systems, highly fluorescent [10] and conducting properties [11,12]. Although extensive studies of these dyes incorporated in LB films have been reported in literature [13,14], little effort has been made to study their nonamphiphilic counterparts especially the carboxyimides in LB films. Nonamphiphilic molecules mixed with fatty acids are capable of forming excellent LB films [15–17] and their spectroscopic and aggregating properties are reported to be similar to their amphiphilic counterparts. These features justify the study of nonamphiphilic molecules assembled in LB films as they eliminate cumbersome synthesizing and purification processes that make the yield of the final products low and extremely expensive and hence unsuitable for large scale applications.

In this article, we report the behavior of nonamphiphilic *N,N'*-bis (2,6-dimethylphenyl)-3,4,9,10-perylenetetracarboxylic diimide, (DMPI) mixed with stearic acid (SA) at the air–water interface and their steady state spectroscopic properties when transferred onto quartz substrates as LB films. Interest in this study stems from our previous and continuing efforts to understand the behavior of nonamphiphilic compounds assembled in LB films and their interaction

* Corresponding author. Tel.: +1-819-376-5077 ext. 3340; fax: +1-819-376-5057; e-mail: ashim_dutta@uqtr.uquebec.ca

1010-6030/98/$19.00
PII S1010-6030(98)00209-3

with the microenvironment in these supramolecular assemblies. Detailed studies reveal an intense, broad and structureless band corresponding to an aggregated dimer of DMPI in these LB films.

2. Experimental details

DMPI was purchased from Aldrich Chemical, Milwaukee, and used as received. SA was obtained from Sigma and used as received. A commercially available Langmuir–Blodgett (LB) deposition trough Joyce-Loebl Trough IV obtained from Joyce-Loebl, Newcastle upon Tyne, UK was used for the deposition of mono- and multilayers. Surface pressure measurements was achieved using a filter paper Wilhelmy plate balance interfaced to a computer that controlled the movements of the barrier at the air–water interface with an accuracy of ± 0.1 mN m^{-1}. The surface pressure vs. area per molecule isotherms were obtained in a conventional manner by spreading at the air–water interface about 100 μl of a chloroform solution of DMPI and SA mixed in a predetermined ratio. After allowing 15 min for the solvents to evaporate, the film formed at the air–water interface was compressed very slowly at a rate of 2×10^{-3} nm^2 mol^{-1} s^{-1}. The subphase used was triple distilled water deionized by a Millipore water deionizing system having a resistivity of 18.2 MΩ cm and pH = 5.6. The reproducibility of the isotherms was checked and found to be well within a permissible experimental error limit of about 5–8%. All isotherms reported in this work is an average of five isotherms recorded under identical conditions. Mixed LB films were deposited on previously cleaned fluorescent grade quartz slides by moving the slides vertically through the floating monolayer at the air–water interface with a speed of 1 mm s^{-1} at a constant surface pressure of 20 mN m^{-1}. The transfer ratio for Y-type deposition of the films was determined to be about 0.91 ± 0.01. The transfer ratio was calculated from the ratio of the area of the substrate coated with the monolayer to the change in actual area of the monolayer at the air–water interface produced due to deposition of the film on the substrate.

Steady state absorption spectra of the mixed LB films were recorded on a Shimadzu UVPC-2010 absorption spectrophotometer, and steady state fluorescence emission was recorded on a Perkin-Elmer MPF-44A spectrofluorimeter. The emission spectra of the LB films deposited on quartz substrates were obtained by front face excitation by placing them on special holders that held the film at an angle of 45° to the source of light and the photomultiplier. Narrow band pass filters (5 nm) were used to minimize the effects of scattering.

3. Results and discussion

3.1. Surface pressure vs. area per molecule isotherms at the air–water interface

A small amount of a solution of DMPI in chloroform (2×10^{-3} M) was spread at the air–water interface and compressed slowly at a rate of 2×10^{-3} nm^2 mol^{-1} s^{-1} after allowing 15 min for the solvents to evaporate. It was observed that the Π-A isotherms collapsed at relatively high surface pressures of about 50 mN m^{-1} but the films could not be transferred on the solid substrates. However, mixed films of SA and DMPI formed excellent floating layers at the air–water interface that could be readily transferred on to quartz substrates with a reasonably good transfer ratio of 0.91 ± 0.01 for Y-type deposition.

Fig. 1 shows the surface pressure (Π) vs. the average area per molecule (A) isotherms of DMPI mixed with SA at different molar ratios. These isotherms closely resemble the isotherm of molecules that form islands at the air–water interface. With increasing mole fraction of DMPI, the average area per molecule decreases (Fig. 2). This is probably indicative of DMPI molecules stacked on top of each other and subsequently pushed out of the air–water interface to remain sandwiched between the fatty acid chains so as not to occupy any area at the air–water interface that accounts for a decrease in the average area per molecule with increasing mole fraction

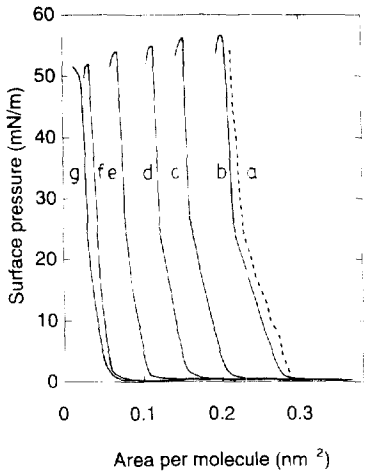

Fig. 1. Surface pressure vs. area per molecule isotherm of DMPI mixed with SA at different mole fractions of DMPI in the mixture at the air–water interface: (a) 0, (b) 0.006, (c) 0.015, (d) 0.028, (e) 0.056, (f) 0.14, (g) 1.0.

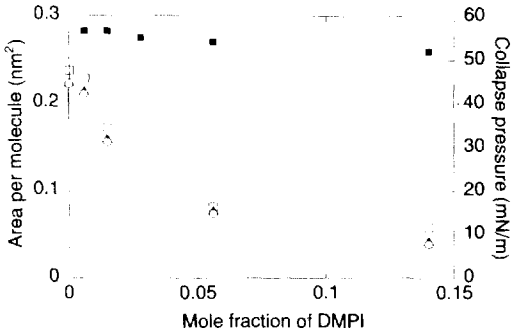

Fig. 2. Plot of the average area per molecule of the mixed films of DMPI and SA at the air–water interface vs. the mole fraction of DMPI in the mixed films at different surface pressures: 10 mN m^{-1} (open circles); 20 mN m^{-1} (open squares); 30 mN m^{-1} (filled triangles). Plot of the collapse pressure vs. the mole fraction of DMPI in the mixed films at the air–water interface shown by filled squares.

of DMPI in the mixed films at the air–water interface. Additionally, the observed average area per molecule of the mixed films is much smaller than that expected for a large molecule like DMPI laying flat at the air–water interface. It therefore appears likely that the DMPI molecules stand on their edge at the air–water interface. Similar behavior has been reported for other nonamphiphilic molecules [16–19]. The alternative trivial possibility of the DMPI molecules being lost in the subphase through submerging was tested using a method discussed elsewhere and was confirmed not to be the case.

Fig. 2 shows a plot of the collapse pressure (Π_c) vs. the mole fraction of DMPI in the mixed films of DMPI and SA at the air–water interface. It is evident from the figure that the collapse pressure changes only slightly with the molar composition of the film confirming immiscibility of the components at the air–water interface in accordance with the phase rule [20–24]. At the air–water interface as a result of interaction with the water molecules, the DMPI and SA get aligned with respect to the air–water interface. While the DMPI–SA interactions tend to produce a homogeneous distribution of the DMPI molecules in the SA matrix the DMPI–DMPI and SA–SA interactions being cohesive in nature and much stronger than the DMPI–SA interactions form aggregates of DMPI and SA [24]. Extensive studies by several workers using different state of art techniques like Brewster angle microscopy [24,25], fluorescence microscopy [26], and atomic force microscopy [27,28] have confirmed the formation of 2D and 3D crystallites [23–28] even at very low dye concentrations justifying the existence of strong cohesive interactions between molecules that assist in the aggregation process.

3.2. Spectroscopic studies of DMPI in solution and in the Langmuir–Blodgett films mixed with stearic acid

Fig. 3 shows the absorption spectra of DMPI in chloroform and in the LB films mixed with SA. In the 400–600 nm spectral region, DMPI in chloroform shows intense absorption bands located at 432 nm, 458 nm, 490 nm with the 0–0 band at 526 nm corresponding to the S_1–S_0 transition that is directed along the long axis of the molecule [48]. The LB film absorption spectrum appears broadened and diffused relative to the solution absorption spectrum with bands located at 468 nm, 498 nm and 538 nm. The 0–0 band in the LB film is located at 538 nm which is red-shifted by about 12 nm relative to that in solution. The overall broadening and red shift of the absorption bands in the LB film may be attributed to the fact that in the LB film both monomers and aggregates of different sizes exist. Unlike in solution the molecules do not have rotational freedom and hence generate sites that are energetically different. The resultant absorption spectrum is therefore a superposition of the spectra of these individual monomers and aggregates that gives rise to a broadened spectral profile.

Fig. 4 shows the emission spectrum of DMPI in chloroform and in the mixed LB films with SA. The solution emission

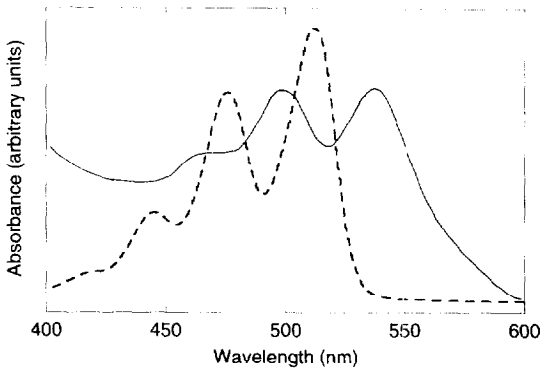

Fig. 3. Absorption spectra of DMPI in chloroform (5×10^{-4} M) shown by short dashed line and 10 layers of the mixed LB films deposited on quartz substrates (molar ratio DMPI:SA being 1:10) shown by a continuous line.

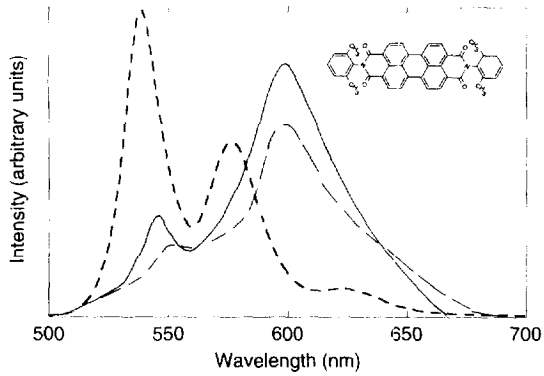

Fig. 4. Emission spectra of DMPI, in chloroform (5×10^{-4} M) shown by a short dashed line and 10 layers of the mixed LB films deposited on quartz substrates (molar ratio DMPI:SA being 1:10) shown by a continuous line and DMPI microcrystals shown by a long dashed line. Inset shows the molecular structure of DMPI.

spectrum in the 500–700 nm region shows the 0–0 band located at 540 nm with the vibronic bands at 575 nm and 625 nm that is in excellent agreement with the spectral characteristics reported for monomeric DMPI [29]. The LB film emission spectrum on the other hand showed large changes. Besides broadening of the monomeric emission band located at 540 nm, an intense and enormously broad excimer-like band with its maximum located at about 597 nm is observed. The origin of the broad excimer-like emission band at 597 nm is not readily explicable. Increasing the concentration of DMPI in solution to 2×10^{-2} M failed to produce the excimer-like broad band emission confirming the absence of highly organized aggregates in solution. Moreover, a detailed comparative study of the absorption and excitation spectra of DMPI in solution and in the LB films, as discussed in a later section confirm that the excimer-like broad band is not a true excimer but is very likely a dimer. Identical observations have been reported for *N,N'*-bis(2,5-di-tert-butylphenyl)-3,4,9,10-perylenedicarboxyimide (DBPI) [30]. According to Ford and Kamat [31] in DBPI, the butylphenyl rings produced steric hindrance to a close approach of the molecules preventing the formation of excimers. The molecular structure [32,33] and spectroscopic characteristics of DMPI

is similar to the DBPI molecule. Given these facts, it does not seem unreasonable that steric hindrance offered by the dimethylphenyl rings may inhibit a close approach of the DMPI molecules resulting in a failure to exhibit the excimer-like emission in solution. On the contrary, in the LB films the broad band excimer-like emission from DMPI molecules is caused as a result of a substantial overlap of the condensed ring systems of neighboring DMPI molecules produced as a result of ordering and specific alignment of the molecules in the LB films. The weak intensity of the band at 540 nm compared to that at 597 nm may be attributed to efficient energy transfer from the monomers to the dimers resulting in the depletion of the monomer fluorescence intensity and enhancement of the dimer fluorescence intensity.

To compare the spectroscopic properties of DMPI aggregates formed in LB films with the microcrystals of DMPI, we have recorded the emission spectrum of DMPI microcrystals. As shown in Fig. 4, the emission profile in the 500–700 nm region is broad and diffused with the maximum located at about 597 nm that is in excellent agreement with the emission characteristics of the LB film. These results confirm the formation of DMPI crystallites in the LB films.

Binary solvent mixtures consisting of components that are completely miscible at all proportions with one of them being an excellent solvent for the solute in contrast to the other which is a poor solvent for the solute constitutes an excellent medium for inducing aggregation. To elucidate better the aggregation process and in an effort to confirm whether or not the aggregates formed by the binary solvent mixtures is identical to the aggregates in the LB films, we have used acetone–water mixtures as an alternate and versatile means of producing aggregates. At low volume fractions of water in the binary mixture of acetone and water, the emission spectrum essentially corresponds to the emission spectrum of DMPI in pure acetone as shown in Fig. 5. With increasing volume fraction of water in the binary solvent mixture the intensity of emission decreases as shown in Fig. 6. It was confirmed that the intensities of the vibronic bands at 539 nm and 576 nm decreased with increasing volume fractions of water in the mixture but the ratio of their intensities remained constant. These results indicate that emission in these systems essentially originate from the monomeric species of DMPI. The overall decrease in fluorescence may however be ascribed to efficient energy transfer from the monomeric species to the aggregates that are nonfluorescent or weakly fluorescent and decay therefrom by nonradiative pathways resulting in the fluorescence quenching of the DMPI monomers. The fact that the ratio of the band intensities at 539 and 576 nm remain constant indicate the absence of reabsorption effects [16–19]. Interestingly, at a volume fraction of 0.8 water (Fig. 6) in the binary solvent mixture a sharp rise in the intensity ratio of the bands is observed that indicates considerable contribution from the excimer-like fluorescence. As mentioned before, this enhancement is attributable to a decrease in the number of monomeric species and to the efficient energy transfer from the monomers to the energetically lower aggregates. Furthermore, this excimer-like emission is broad, diffused and overlaps with the monomeric emission band at 576 nm, adding to its intensity that is plausibly manifested as an enhancement of the intensity ratio of the bands. At still higher volume fractions of water (≥ 0.9) in the binary solvent mixtures, the 0–0 band at 539 nm corresponding to the monomer fluorescence totally disappears and only a broad and diffused band with its band maximum at 597 nm is observed (Fig. 5) that corresponds to the dimer band. Interestingly, the emission spectra of the aggregates formed in the LB films and in the binary solvent mixtures appear to be similar suggesting that the molecular structure of the aggregates formed in the two different systems are probably similar. One plausible explanation seems to be the influence of hydrophobic forces that drive the aggregation process in both the systems. Although monomers of DMPI may still exist, their population is expected to be low and efficient energy transfer from these monomeric sites to the aggregates result in an enhancement of the excimer-like emission and quenching of the monomer emission. Detailed studies of the excitation spectra corresponding to the emission from the aggregates in the LB films, binary mixtures of acetone–water and microcrystals as will be discussed in Section 3.3 confirm different packing configurations of DMPI in the aggregates formed in the different systems.

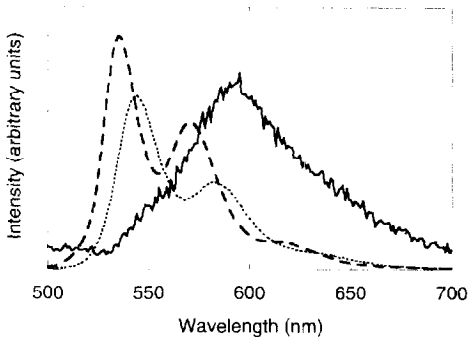

Fig. 5. Emission spectra of DMPI in acetone (3×10^{-4} M) shown by thick short dashed line; in acetone–water binary mixture with 0.6 volume fraction of water (dotted line); in acetone–water binary mixture with 0.9 volume fraction being water shown by thick continuous line.

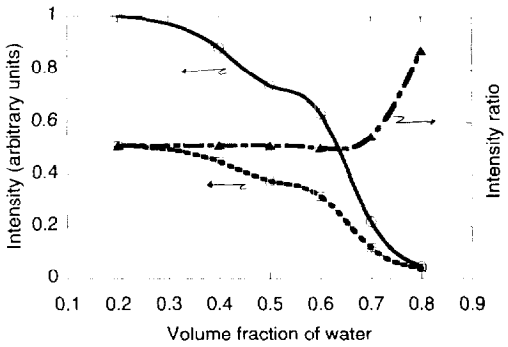

Fig. 6. Plot of the intensities of the emission bands at 539 nm (open circles) and 576 nm (open squares) vs. the volume fraction of water in the binary solvent mixtures of acetone and water. The ratio of the band intensities (I_{576}/I_{539}) vs. the volume fraction of water in the binary solvent mixtures is also shown in the figure by filled triangles.

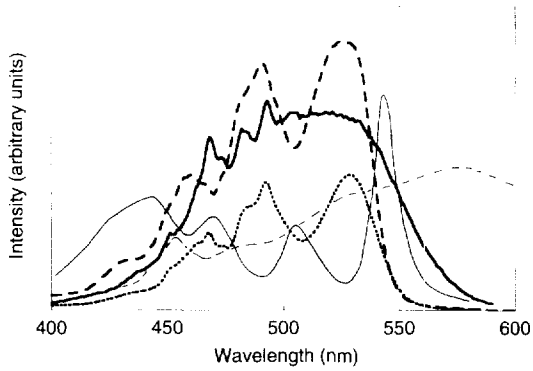

Fig. 7. Excitation spectra of DMPI in chloroform (dotted line); in binary mixture of acetone with volume fraction of water in the mixture equal to 0.9, (short dashed line) λ_{em} = 575 nm in both cases; in 10 layers of the mixed LB film (DMPI:SA = 1:10) (thin continuous line) λ_{em} = 545 nm and (thin dashed line) for λ_{em} = 610 nm; in microcrystals (thick continuous line) λ_{em} = 590 nm.

3.3. Excitation spectra of DMPI in solution, mixed LB films with SA, binary solvent mixtures and microcrystals

Fig. 7 shows the excitation spectrum of DMPI in chloroform in the 400–600 nm spectral region with bands at 467 nm, 493 nm and the 0–0 band located at 527 nm when the emission was monitored at the emission maximum at 575 nm. These results are in excellent agreement with the absorption data. The LB film excitation spectrum with the emission monitored at about 610 nm yielded a band in the 400–600 nm region with the band maximum at about 580 nm. The excitation spectrum corresponding to the monomer band in the LB films yielded a structured band system with an intense 0–0 band at 544 nm, when the emission was monitored at 550 nm. Such large differences in the excitation spectra clearly suggest that the emission at 597 nm is not due to a true excimer but a dimer [34,35]. The excitation spectrum of DMPI in the binary solvent mixtures show the 0–0 band at 526 nm while in case of DMPI microcrystals the 0–0 band is located at 560 nm. Careful examination of the excitation spectra corresponding to the excimer-like emission observed for the aggregates formed in the LB films and in the binary solvent mixtures confirmed them to be also different suggesting different packing configurations of the DMPI molecules in the aggregates formed in the two different systems that establish the role of microenvironment in modifying the aggregation process. Indeed such a possibility seems reasonable as the dimethylphenyl ring is connected to the perylenecarboxyimide system by a single bond about which rotation is possible and hence different overlap configurations of the DMPI molecules in the LB films may result in producing different emission and excitation spectra [30].

4. Conclusions

Briefly, nonamphiphilic DMPI form stable films with SA at the air–water interface that are easily transferred onto solid substrates as LB films which exhibit interesting photophysical properties. The LB film absorption spectrum appears broad, diffused and red shifted compared to that in solution indicating the existence of strong ground state interaction between molecules in the film arising from aggregation of the DMPI molecules in the LB film. Sharply in contrast to the structured fluorescence emission from DMPI in solution, the fluorescence emission from the mixed LB film is broad, diffused and structureless with two bands, one corresponding to the monomer band located at 540 nm and the other excimer-like emission at 597 nm originating from the small aggregates or crystallites of DMPI. Interestingly, such an excimer-like emission is never revealed in solution as the dimethylphenyl rings are oriented with their planes perpendicular to the plane of the perylenetetracarboxylic diimide chromophore preventing a close approach of neighboring moieties. In LB films, highly organized small aggregates or crystallites are formed that is spectrally manifested as a broad band with its maximum at 597 nm. One plausible explanation could be the rotation of the dimethylphenyl ring relative to the perylenedicarboxylic diimide group permitting a close approach of the DMPI molecules. Interestingly, similar aggregates may be simulated by using a binary solvent mixture. Although the emission spectrum in all cases appears similar, a comparison of the excitation spectra of DMPI in these systems confirm that the packing configuration of the DMPI molecules in the different systems are indeed different that probably reflects the different interaction between the DMPI molecule with its microenvironment.

Acknowledgements

The author would like to express his thanks to Prof. T.N. Misra, Department of Spectroscopy, Indian Association for the Cultivation of Science, Calcutta, India for providing all possible laboratory facilities for this work.

References

[1] A. Ulman, An Introduction to Ultrathin Organic Thin Films: From Langmuir–Blodgett Films to Self-Assemblies, Academic Press, New York, 1991.
[2] P.N.Prasad, D.J. Williams, Non-linear Optical Effects in Molecules and Polymers, Wiley, New York, 1991.
[3] J.D. Swalen, D.L. Allara, J.D. Andrade, E.A. Chandross, S. Garoff, J. Israelachivili, T.J. McCarthy, R. Murray, R.F. Pease, J.F. Rabolt, K.J. Wynne, H. Yu, Langmuir 3 (1987) 932.
[4] F.L. Carter, Molecular Electronic Devices II, Marcel-Dekker, New York, 1987.
[5] T. Tsuzuki, N. Hirota, N. Noma, Y. Shirota, Thin Solid Films 273 (1996) 177.
[6] S. Hamm, H. Wachtel, J. Chem. Phys. 103 (1995) 10689.
[7] C. Goltner, D. Pressner, K. Mullen, H.W. Speiss, Angew. Chem., Int. Ed. Engl., (1993) 32.
[8] Y. Toda, H. Yanagi, Appl. Phys. Lett. 69 (1996) 2315.
[9] J. Duff, A.M. Hor, A.R. Melnyk, D. Teney, SPIE Hard Copy Printing Mater. Media Process 1253 (1990) 184.

[10] H.G. Lohmansroben, H. Langhals, Appl. Phys. B. 48 (1989) 449.
[11] V. Bulovic, P.E. Burrows, S.R. Forrest, J.A. Cronin, M.E. Thompson, Chem. Phys. 210 (1996) 1.
[12] V. Bulovic, S.R. Forrest, Chem. Phys. 210 (1996) 13.
[13] R. Aroca, E. Johnson, A.K. Maity, Appl. Spectrosc. 49 (1995) 466.
[14] E. Johnson, R. Aroca, Appl. Spectrosc. 49 (1995) 472.
[15] H. Kuhn, Thin Solid Films 99 (1983) 1.
[16] A.K. Dutta, T.N. Misra, A.J. Pal, J. Phys. Chem. 98 (1994) 4365.
[17] A.K. Dutta, J. Phys. Chem. 99 (1995) 14758.
[18] A.K. Dutta, Langmuir 12 (1997) 5909.
[19] A.K. Dutta, J. Phys. Chem. 98 (1994) 12844.
[20] G.L. Gaines, Jr., Insoluble Monolayers at Liquid–Gas Interfaces, Interscience Publishers, New York, 1966.
[21] W. Rettig, H.D. Dörfler, Mater. Sci. Forum 25–26 (1988) 577.
[22] A.W. Adamson, Physical Chemistry of Surfaces, Wiley-Interscience, New York, 1990.
[23] H.D. Dorfler, Adv. Colloid Interface Sci. 31 (1990) 1.
[24] A. Angelova, M. Van der Auweraer, R. Ionov, D. Vollhardt, F.C. DeSchryver, Langmuir 11 (1995) 3167.
[25] G.A. Overbeck, D. Honig, D. Mobius, Langmuir 9 (1993) 555.
[26] R.M. Weiss, M. McConell, Nature 310 (1984) 47.
[27] E.T. Grotenhuis, J.C. Van Miltenburgh, J.P. Van Eerden, Chem. Phys. Lett. 261 (1996) 558.
[28] A.K. Dutta, Langmuir 13 (1997) 5678.
[29] R. Gvishi, R. Reisfeld, Z. Burshtein, Chem. Phys. Lett. 213 (1993) 338.
[30] A.K. Dutta, K. Kamada, K. Ohta, Langmuir 12 (1996) 4158.
[31] W.E. Ford, P.V. Kamat, J. Phys. Chem. 91 (1987) 6373.
[32] F. Graser, E. Hadicke, Acta Cryst. C 42 (1986) 189.
[33] G. Kelbe, F. Graser, E. Hadicke, E. Berndt, J. Acta Cryst. B 45 (1989) 69.
[34] F.M. Winnik, Chem. Rev. 93 (1993) 587.
[35] J.B. Birks, Photophysics of Aromatic Molecules, Wiley- Interscience, London, 1970.